

Published in final edited form as:

Cancer Prev Res (Phila). 2012 April ; 5(4): 562–573. doi:10.1158/1940-6207.CAPR-11-0502.

Metformin prevents the development of oral squamous cell carcinomas from carcinogen-induced premalignant lesions

Lynn Vitale-Cross¹, Alfredo A. Molinolo¹, Daniel Martin¹, Rania H. Younis², Takashi Maruyama^{3,4}, Vyomesh Patel¹, Wanjun Chen³, Abraham Schneider^{2,*}, and J. Silvio Gutkind^{1,*}

¹Molecular Carcinogenesis Section, Oral and Pharyngeal Cancer Branch (L. V.-C., A.A.M., J.S.G.), National Institute of Dental and Craniofacial Research, National Institutes of Health, Bethesda, Maryland. ²Department of Oncology and Diagnostic Sciences, School of Dentistry (R.H.Y., A.S.) and Greenebaum Cancer Center, Program in Oncology, University of Maryland, Baltimore, Maryland (A.S.). ³Oral Mucosal Immunology Section, Oral Infection and Immunity Branch (T.M., W.C.), National Institute of Dental and Craniofacial Research, National Institutes of Health, Bethesda, Maryland.

Abstract

Head and neck squamous cell carcinoma (HNSCC) is a major public health concern. The recent identification of the mammalian Target of Rapamycin Complex 1 (mTORC1) signaling pathway as a highly prevalent molecular signature underlying HNSCC pathogenesis has provided the foundation to search for novel therapeutic approaches to prevent and treat HNSCC. Here, we asked whether metformin, the most widely used medication for the treatment of type 2 diabetes, which acts in part by stimulating the AMP-activated protein kinase (AMPK) signaling pathway thereby reducing mTORC1 activity, may lower the risk of HNSCC development. Indeed, we show that metformin reduces the growth of HNSCC cells and diminishes their mTORC1 activity by both AMPK-dependent and –independent mechanisms. We also optimized an oral-specific carcinogenesis mouse model that results in the accumulation of multiple oral premalignant lesions at the end of the carcinogen exposure, some of which then spontaneously progress into HNSCC. Using this mouse model, we observed that metformin specifically inhibits mTORC1 in the basal proliferating epithelial layer of oral premalignant lesions. Remarkably, metformin prevented the development of HNSCC by reducing significantly the size and number of carcinogen-induced oral tumoral lesions, and by preventing their spontaneous conversion to squamous cell carcinomas. Collectively, our data underscore the potential clinical benefits of using metformin as a targeted chemopreventive agent in the control of HNSCC development and progression.

Keywords

Oral cancer; premalignant lesions; targeted therapy; mTOR

INTRODUCTION

Head and neck squamous cell carcinoma (HNSCC), most of which arise mostly in the oral cavity, continues to be a major public health concern. In 2011, more than 49,200 new cases

*Co-Corresponding Authors: A.S., aschneider@umaryland.edu; and J.S.G., sg39v@nih.gov.

⁴Current address Laboratory of Cell Recognition and Response, Graduate School of Life Sciences, Tohoku University, Aoba 6-3, Aramaki, Aoba-ku, Sendai, 980-8578, Japan.

of HNSCC will be diagnosed, and 11,400 deaths are predicted to occur from this disease in the United States alone (1). The recent identification of the PI3K, Akt, and mammalian Target of Rapamycin Complex 1 (mTORC1) signaling pathway as a highly prevalent molecular signature underlying HNSCC pathogenesis (2-8) has provided the foundation to search for novel molecular-targeted strategies to halt the disease process.

In HNSCC, the activation of mTORC1 may result from the overactivity of EGFR, which is often aberrantly overexpressed in HNSCC thereby causing the phosphorylation and activation of the lipid kinase PI3K, or by the downregulation of the expression of the tumor suppressor protein PTEN, which acts as a lipid phosphatase inhibiting the accumulation of the PI3K enzymatic product, PIP₃ (reviewed in (9)). Alternatively, PIP₃ levels can be raised by the presence of activating mutations in *PI3K* and the *ras* oncogene, and by inactivating mutations in the *Pten* tumor suppressor gene, all of which have now been established to occur in a non-overlapping fashion in HNSCC (6, 7). The accumulation of PIP₃ stimulates the kinase Akt, which inactivates the tumor suppressor protein complex TSC1/TSC2 (10), leading to the accumulation of active GTP-bound Rheb, which in turn activates mTOR (10) as part of the conserved kinase complex mTORC1 (11). The mTORC1 oncogenic network supports a progressive metabolic reprogramming that favors cancer cell macromolecular biosynthesis, proliferation, survival and ultimately metastasis (11). Indeed, recent analysis of the HNSCC genomic landscape indicates that the accumulation of mutations in the Akt/mTOR pathway may represent the most prominent oncogenic driver in HNSCC (6, 7), thus providing the genetic basis for current efforts aimed at targeting mTOR in this highly prevalent malignancy.

Of interest, this emerging information suggests that the use of mTORC1 inhibitors, such as sirolimus (*aka.* rapamycin), everolimus (RAD001) or temsirolimus (CCI-779) could be explored for preventing HNSCC progression. However, their potential immunosuppressive activity and other dose-dependent side effects may raise safety concerns regarding the long term use of rapamycin and derivatives (rapalogs) as chemopreventive agents in patients diagnosed with premalignant oral lesions, where only 10-15% of which are expected to progress to HNSCC overtime (12-14). In this regard, recent studies indicate that metformin, the most widely used drug in the United States for the treatment of type 2 diabetes, may lower the risk of cancer and/or improve cancer prognosis (12-14). Approximately 120 million people use metformin worldwide (15), and compelling evidence demonstrates that metformin treatment can reduce tumor cell growth in part by reducing mTORC1 activity (reviewed in 16). These inhibitory effects appear to be controlled by the AMP-activated protein kinase (AMPK) signaling pathway, a key sensing mechanism of cellular bioenergetics (17, 18). As a mild inhibitor of mitochondrial complex I, metformin induces AMPK activation following the inhibition of oxidative phosphorylation, which leads to an increase in cellular AMP levels (19) and the consequent activation of AMPK after its phosphorylation by the serine/threonine kinase LKB1 (20). AMPK phosphorylates and activates TSC2, hence antagonizing the small GTPase Rheb and reducing mTORC1 activity (21). Therefore, in malignancies where the mTORC1 pathway is frequently hyperactivated, such as HNSCC, targeting AMPK activation by metformin appears highly desirable.

Here, we show that metformin treatment inhibits mTORC1 activation in representative human-derived HNSCC cell lines, and confirmed that metformin triggers AMPK pathway activation and prevents tumor cell proliferation in these HNSCC cells. However, we observed that the inhibitory action of metformin on mTORC1 activity appears to occur via an AMPK independent mechanism. This was observed in both HNSCC cells after LKB1 knock down, and in HeLa cells where *LKB1* is mutated and inactive. Encouraged by these results, we optimized a recently established oral-specific carcinogenesis mouse model aimed at exploiting it to examine the ability to halt the conversion of oral premalignant lesions into

HNSCC (22). We demonstrate mTORC1 inhibition by metformin occurs primarily in the basal proliferating layer of oral premalignant lesions, as evidenced by the hypophosphorylation of the ribosomal protein S6, a common mTORC1 downstream surrogate marker. Remarkably, metformin prevented the development of HNSCC by significantly reducing the size and number of carcinogen-induced oral tumoral lesions, and by preventing their spontaneous conversion to squamous cell carcinomas. Collectively, our data underscores the potential clinical use of metformin as a targeted chemopreventive agent in the control of HNSCC development and progression.

MATERIALS AND METHODS

Reagents, cell lines, tissue culture, and transfections

4-nitroquinoline-1-oxide (4NQO; Sigma-Aldrich) was added to the drinking water to a final concentration of 50 µg/ml. Metformin (Spectrum Chemical) was diluted in sterile saline and administered to mice by intraperitoneal (i.p.) injections at a dose of 50 mg/kg/day. HaCat cells (a non-transformed skin keratinocyte cell line), human-derived HNSCC cell lines Cal-27, HN12, HN13, and Hep2 (2), and cervical SCC HeLa cells were grown and maintained as described in Supplemental Material, and underwent DNA authentication (Genetica DNA Laboratories, Inc.) to ensure consistency in cell identity in comparison with their source. RNA interference experiments were performed in cells transfected with commercially available LKB1 siRNAs (Qiagen), HiPerfect transfection reagent (Qiagen) and serum-free, antibiotic-free DMEM at a final concentration of 25 nM as previously described (23). Two LKB1 target sequences were used: Hs_STK11_5 and Hs_STK11_7. All Starts siRNA (Qiagen) served as the non-targeted control. Cells were treated with metformin at the indicated dose and time, using rapamycin (LC Laboratories) as a control. See Supplemental Material for additional details.

Western blotting, cell proliferation and viability assays, and ATP assay

Immunodetection was performed as previously described (2), using antibodies from Cell Signaling Technology against phospho-S6 Ser240/244, ribosomal protein S6, phospho-acetyl-CoA carboxylase (Ser79), phospho-AMPKα (Thr172), phospho-4E-BP (T37/46), 4E-BP, non-Phospho-4E-BP (T46), p70S6K, phospho-p70S6K, and LKB1. Mouse monoclonal anti-tubulin was purchased from Santa Cruz. For proliferation assays, cells were grown in 24-well plates and incubated with 0.5 µCi [³H]-thymidine/ml (Perkin Elmer) for the last 4 hours of treatment, lysed, and radioactivity incorporated into cellular DNA counted in a liquid scintillation counter. For viability assays, the CellTiter 96® AQueous One Solution (MTS) reagent was used following the manufacturer's protocol (Promega) as previously described (24). Cellular ATP levels were assessed by using an ATP assay kit (Calbiochem) as previously described (25). See Supplemental Material for additional information.

Experimental animal model, and plasma levels of IGF-1 and insulin

All animal studies were carried out according to NIH-approved protocols, in compliance with the Guide for the Care and Use of Laboratory Animals. Female C57Bl/6 mice 4 to 6 week-old were given either water (control) or 4NQO in the drinking water for the indicated time, and then reverted to regular water and monitored until week 22. All animals underwent a biweekly full oral cavity examination under anesthesia, and euthanized at the indicated time points for tissue retrieval. Tissues were fixed, and processed for paraffin embedding for histopathological diagnosis and further immunohistochemical studies (22). For the analysis of the effect of metformin on tumor development, mice were exposed to 4NQO for 14 weeks and randomly distributed into treatment and control groups, which received daily i.p. injections with metformin (50 mg/kg/day) or an equal volume of diluent (sterile saline). All animals were euthanized on week 22, and tissue retrieval was performed as described above.

Mice were sacrificed 2 hs after the last administration of metformin, and plasma levels of IGF-1 and insulin were determined using the Abnova Igf1 (Mouse) ELISA Kit and Millipore mouse insulin ELISA kit, respectively, following the manufacturer instructions. See Supplemental Material for additional information.

Immunohistochemistry, immunofluorescence

Anti phospho-S6 (Ser235/236) (#2211S) (Cell Signaling Technology), anti-cytokeratin 5 (Thermo Scientific) (MS-1896-R7), anti-Ki-67 anti-mouse antibody (DAKO) (M7249) were used for immunohistochemical analysis of paraffin sections as described (22) (see Supplemental Material) Stained slides were scanned using an Aperio CS Scanscope (Aperio, CA, USA) and quantified using the available Aperio algorithms. For immunofluorescence studies, tissue sections were processed as described (22), and mounted with Vectashield (Vector Laboratories). See Supplemental Material for additional information.

T cell proliferation assay and flow cytometry

Spleen cells (5×10^4 cells) from 4NQO metformin-treated or 4NQO control mice were cultured in the presence or absence of anti-CD3 antibody (0.5 mg/ml). The cultured cells were pulsed [^3H]-thymidine for the final 16 hours, collected, and radioactivity measured as above. Flow cytometric analysis was performed as described before (26). Cells were stained with antibodies to indicated surface markers followed by intracellular cytokine antibodies using the BD Cytofix/Cytoperm kit (BD Biosciences). Foxp3 staining was performed according to the manufacturer's instruction (eBioscience). The following fluorescein-conjugated anti-mouse antibodies were purchased from BD Biosciences: anti-IFN- γ , anti-CD4, anti-CD8, anti-Foxp3, as well as their respective isotype control antibodies. Anti-IL-17 was purchased from BioLegend.

Statistical analysis

ANOVA followed by the Tukey t test were used to analyze the differences between groups after treatments. Data analysis was done using GraphPad Prism version 5.01 for Windows (GraphPad Software); P values of <0.05 were considered statistically significant. Two-tailed, unpaired t tests were used to analyze the differences in tumor growth between experimental groups, as well as differences in Ki-67 expression and low and high grade dysplasia between treated and control groups.

RESULTS

Metformin treatment inhibits HNSCC cell proliferation

Metformin exerts an antiproliferative effect in cultured tumor cells derived from a variety of human cancers (18, 27, 28). To determine whether metformin impairs HNSCC cell proliferation, increasing doses of the drug were used to treat HN12 cells (Figure 1A), a representative HNSCC cell line that is sensitive to the anti-tumoral effect of mTORC1 inhibition (2). A significant reduction in tumor cell proliferation, as determined by [^3H] thymidine incorporation, was evident following treatment with the 10 mM and 20 mM doses. A similar growth inhibitory activity was observed in other HNSCC cell lines (Figure S1A). Noteworthy, while metformin triggered a marginal decrease in cell viability in non-transformed HaCat keratinocytic cells, a similar dose-dependent decline in cell viability was observed in other HNSCC cell lines including HN13 and Hep2 cells (Figure S2). Metformin also induced a significant reduction in HN12 cell viability when assessed daily for 4 days (Figure 1B).

mTORC1 pathway activity is downregulated by metformin through an AMPK-independent mechanism

Metformin treatment leads to AMPK activation following a cellular bioenergetic crisis that increases the AMP/ATP ratio (29). In this regard, we observed that following treatment of HN12 cells with metformin, the expression levels of phosphorylated AMPK α (Thr172) (pAMPK α) and its downstream target ACC (pACC) were upregulated in a dose-dependent manner (Figure 1C). Not surprisingly, activation of AMPK signaling following metformin also resulted in a dose-dependent, concomitant reduction in mTORC1 activity, as judged by the hypophosphorylated status of ribosomal protein S6 (pS6) (Figure 1C), and the mTOR downstream targets p70S6K and 4E-BP (Figure S1). As depicted in Figure 1D, AMPK α phosphorylation increased within 15 minutes following treatment with metformin, reached its peak at 2 hours and decreased thereafter, suggesting a direct correlation between pAMPK levels with the ongoing bioenergetic crisis. Indeed, metformin-treated HN12 cells demonstrated a dramatic drop in cellular ATP levels when compared to untreated cells (Figure S3). These events began relatively early after adding metformin (30 min) and lasted for at least 8 hours. A similar response was evident with 2-DG, a positive control used to mimic energy stress. However, it was noticeable that while no pAMPK levels were detected at 16 hours and 24 hours following metformin treatment, the phosphorylated status of ribosomal protein S6, started to decrease at about 8 hours and remained down for at least 24 hours. These unexpected findings suggested either a long-lasting effect of metformin-induced AMPK activation or the potential influence of alternative mechanisms driving mTORC1 inhibition in response to cellular energy stress.

To examine whether AMPK activation plays an indispensable role on mTORC1 pathway inhibition in HNSCC cells treated with metformin, we decided to knock down LKB1, the main upstream serine/threonine kinase responsible for driving AMPK activation and decreasing gluconeogenesis in the liver in response to metformin (20). Interestingly, we found that in LKB1-depleted HN12 cells, metformin treatment significantly reduced the levels of phosphorylated S6 to a similar extent as the control siRNA-transfected cells, suggesting that in HNSCC, metformin-induced mTORC1 inhibition occurs through signaling mechanisms that are independent of the LKB1/AMPK pathway (Figure 1E). We confirmed these findings in experiments using HeLa cells, which exhibit endogenous impaired LKB1 activity as a result of complete methylation of the *LKB1* promoter region (30). In this regard, we found that in the absence of AMPK activation, metformin treatment led to a marked decrease in mTORC1 activity and tumor cell proliferation, respectively (Figure 1F, and Figure S1 and S3). Overall, these data suggest that metformin might trigger a stress response driven by an alternative, AMPK independent signaling mechanism to cope with the ongoing cellular energetic crisis.

Optimization of the oral chemical carcinogenesis model using 4NQO to study the conversion of oral premalignant lesions into squamous cell carcinomas

We have recently demonstrated that through the use of an oral-specific carcinogenesis model induced by low dose 4-nitroquinoline-1 oxide (4NQO) in the drinking water, immunocompetent C57Bl/6 mice inevitably developed oral squamous cell carcinomas (22). 4NQO is a synthetic water-soluble chemical carcinogen that forms DNA adducts, causes adenosine for guanosine substitutions, and induces intracellular oxidative stress resulting in mutations and DNA strand breaks, all similar to the genetic alterations provoked by tobacco carcinogens, and hence 4NQO often serves as a surrogate for tobacco exposure (31). Emerging studies from our and other groups suggest that this animal model may provide a predictable preclinical strategy to mimic human HNSCC carcinogenesis, which can be used to investigate the efficacy of novel therapeutic approaches for HNSCC treatment (31). However, using this experimental approach most mice exhibit 1-3 carcinomas together with

multiple dysplastic lesions at the end of the carcinogen exposure, thus limiting the ability to examine the benefit of preventive agents unless they also display anticancer properties. In the present study, we first decided to perform an optimization protocol to study the conversion of potential oral premalignant lesions (i.e., epithelial dysplasias) into squamous cell carcinomas, hence affording the opportunity to explore novel chemopreventive strategies to halt tumor progression.

To this end, C57Bl6 mice were exposed to 4NQO in the drinking water either for 8, 10, 12, 14 or 16 weeks (Figure 2A). Within each of the groups, half of the mice were euthanized following termination of the 4NQO administering period, whereas the other half of the remaining mice were reverted to regular water and evaluated until week 22. Examples of gross anatomical appearance and histological features of tumoral lesions appearing in the tongue of 4NQO treated mice are shown in Figure 2B. At each time point, detailed histological analysis revealed the presence of multiple low-grade epithelial dysplasias in all mice exposed to 4NQO for at least 8 weeks. However, mice began accumulating high-grade dysplasias (2-3 lesions per mouse) only after 12 weeks of oral carcinogen treatment (Figure 2A). This dependence on carcinogen exposure was clearly reflected in the number of squamous carcinomas after 22 weeks from the initiation of 4NQO administration. None of the animals exposed to 4NQO for 8 weeks developed malignant lesions, while very few of the mice treated for 10 weeks developed squamous carcinomas at this time point (week 22). When analyzed after 22 weeks, the average number of malignant lesions was 0.5 in mice treated with 4NQO for 12 weeks, while most of the mice had at least one squamous cell carcinoma if treated with the chemical carcinogen for 14 weeks, and exhibited multiple carcinomas after treating for 16 weeks (Figure 2A). Thus, while 4NQO exposure for 12-16 weeks causes primarily epithelial dysplasias, these lesions continue to progress into squamous cell carcinomas even after switching to regular water not containing 4NQO, underscoring the long-lasting effects of 4NQO on oral epithelial tissues. These findings suggest that 4NQO initially triggers genetic alterations in oral epithelial cells that result in the development of mainly premalignant lesions, which can then spontaneously progress into carcinomas. Indeed, the carcinogen 4NQO may be regarded as a surrogate of tobacco exposure, as judged by the striking gross and histopathological resemblance of 4NQO-induced oral carcinogenesis to the premalignant and malignant lesions commonly observed in humans (Figure 2B). For practical purposes, based on this analysis we selected for further studies the inclusion of 4NQO in the drinking water for 14 weeks, as the ratio of the number of squamous carcinomas after 22 weeks with respect to the average number of potential premalignant lesions at the end of the carcinogen exposure is approximately 1:7, which is similar to the rate of conversion of human potential premalignancies into carcinomas (32).

Metformin reduces the size and number of oral tumors induced by 4NQO, and halts the progression of potential premalignant lesions

We next asked whether treating mice with metformin may prevent HNSCC progression, and if so, whether inhibition of the mTORC1 pathway may contribute to the tumor growth inhibitory responses. Following a 14-week exposure to 4NQO in the drinking water, mice were randomly assigned to receive daily administration of metformin (50 mg/kg/day) or an equal volume of sterile saline (control group) for 8 weeks. During this 8-week period, mice were reverted to drinking water only. While the number and size of oral lesions in the control mice increased in a time-dependent manner, a significant reduction in these parameters was initially evident in the metformin group after 4 weeks of treatment (week 18) and remained lower until the conclusion of the experimental period (week 22) (Figure 3A). By week 22, mice exposed to 4NQO predictably developed visible and palpable irregular, whitish, papillary-like oral tumors mainly localized on the tongue. Conversely, the

number and sizes of the visible oral lesions were significantly decreased in mice that were treated with metformin (Figure 3B-D).

Histological examination of all oral lesions at week 22 of control and metformin treated mice after exposure to 4NQO for 14 weeks revealed a striking impact of metformin in tumor progression (Figure 4A-H). In particular, while metformin reduced the overall number of benign and malignant tumor lesions to less than half of those observed in the control group (Figure 4E), it nearly abolished the progression to squamous cell carcinomas, with a single malignant lesion within the group of treated mice, while most control mice exhibited one to two cancer lesions (Figure 4F). We also observed a significant decrease in the number of low and high grade dysplasias after metformin treatment (Figure 4G and 4H). These results indicate that systemically administered metformin apparently hampered the progressive increase in the number and size of oral lesions, suggesting a potential interference of the neoplastic transformation process induced by 4NQO exposure.

Metformin exerted a very limited impact on serum components and metabolic markers (Table 1) as well as in the plasma levels of insulin and IGF-1 (Figure S4). We also investigated whether metformin treatment affected immune responses in mice. We showed that metformin decreased slightly the frequency of both CD4⁺ and CD8⁺ T cells in the spleens compared with the control mice (Table 1). However, T cell proliferation of splenic cells was surprisingly increased in response to T cell receptor stimulation with CD3-specific antibody (Table 1). This suggests the T cell proliferative response per se was not reduced, but rather enhanced, considering the decreased frequency of T cells in the spleen. We next compared the T cell subsets in the mice treated with metformin with those in control mice and showed that metformin significantly enhanced Th17 cells without changing Th1 and Foxp3⁺ Tregs (Table 1). These data together indicate that metformin treatment does not lead to immunosuppression, rather it might enhance the potential of T cell proliferation and differentiation.

Metformin decreases mTORC1 activity in the basal layer of dysplastic squamous lesions

Metformin treatment decreased the basal proliferation of hyperplastic regions in the tongue of 4NQO treated mice (Figure 5A). In this regard, emerging studies indicate that metformin may lower the risk of cancer and/or improve cancer prognosis in part by inhibiting the mTORC1 pathway (16). Hyperactivation of the mTORC1 signaling pathway is a frequent event in HNSCC, playing an important role in promoting carcinogenesis, as judged from studies in human HNSCC and in the murine 4NQO carcinogenic model (2, 4, 9, 22). In spite of the persistent activation of the mTORC1 pathway in this cancer type, the effects of metformin on this major oncogenic signaling pathway remains unexplored. By the immunohistochemical analyses against the phosphorylated form of S6, pS6, we confirmed previously reported findings by our group supporting that pS6 immunoreactivity is clearly restricted to the upper non-proliferating parabasal epithelial cell layer, while basal and suprabasal cells lack positive staining in normal lingual mucosa derived from normal control mice as well as in 4NQO-induced hyperplastic lingual lesions (Figure 5B) (22). Although a similar pattern of pS6 immunostaining was detected in 4NQO-induced dysplastic lesions, it was noticeable that a considerable number of basal and suprabasal cells were pS6 positive (Figure 5B). In contrast, pS6 is clearly positive in most cells in oral SCC, as we have observed in a large number of human HNSCC lesions (3), and in the 4NQO-induced oral cancer experimental model (Figure 5B, right panel). Thus, it appears reasonable to imply that a progressive dysregulation of the mTORC1 pathway occurs early in the carcinogenic process, with basal proliferating epithelial cells exhibiting mTORC1 activation, a process that then may become an intricate event driving the malignant conversion of premalignant lesions.

In this regard, an interesting finding was the observation that pS6 immunoreactivity in dysplastic lesions derived from 4NQO-exposed mice treated with metformin showed a highly significant reduction in the number of basal and suprabasal cells demonstrating positive pS6 reactivity. Similar observations were noticed when immunofluorescence stainings in normal lingual mucosa and dysplastic lesions were performed against pS6 and keratin 5 (K5), a ubiquitous keratin commonly localized in the basal and suprabasal layers of the oral epithelium. As shown in Figure 5C, metformin treatment was able to significantly reverse the increase in pS6 reactivity observed in the basal cells of dysplastic lesions of control-treated 4NQO mice.

Overall, these results systematically demonstrate that metformin deters carcinogen-induced HNSCC development and progression, most likely through the inhibition of mTORC1 activity within a dysplastic epithelial niche occupied by proliferating basal and suprabasal cells. These compelling findings imply that the use of metformin to block the activity of this major oncogenic pathway early in the carcinogenic process may offer a promising chemopreventive strategy to control the development of a cancer type where locoregional invasion, nodal metastasis and chemoresistance are hallmarks of advanced disease and poor patient survival (33).

DISCUSSION

The identification of the mTORC1 signaling network as frequently hyperactivated early in the carcinogenic process, including preneoplastic lesions, and in fully established HNSCC points to this major oncogenic pathway as a potential target to deter disease progression (2-5). Indeed, we have recently demonstrated that chronic administration of rapamycin prevents the malignant conversion of tumoral lesions and promotes the regression of advanced carcinogen-induced HNSCCs that developed in mice receiving prolonged administration of 4NQO in the drinking water (22). Despite these promising results, it should be taken into consideration that from a chemopreventive perspective, utilization of a drug such as rapamycin, which can exert immunosuppressive and other undesirable systemic side effects (i.e. thrombocytopenia and hyperlipidemia), may not represent the best option to chronically target low risk patients exhibiting epithelial dysplasia. To this end, it is imperative that chemoprevention protocols must incorporate pharmacological agents with proven efficacy, which should also include a well-established record of tolerability, safety and minimal toxicity (34). Here, we demonstrate that chronic treatment with metformin, the most widely used oral antidiabetic worldwide, hindered the progression of 4NQO-induced preneoplastic lesions demonstrating low- and high-grade dysplastic lesions, thus supporting the potential use of metformin for HNSCC chemoprevention.

Metformin reduced the mTORC1 activity in the basal layer of oral cancer premalignant lesions, which is likely to harbor the precursors of the HNSCC tumor initiating cells. However, the precise mechanism by which metformin diminishes mTORC1 activity both *in vitro* and *in vivo* is still unclear, and likely involves multiple complementary molecular processes. For example, metformin can reduce the circulating levels of insulin and insulin like growth factor 1 (IGF-1) (35), which could impact on the growth potential of premalignant oral epithelial cells *in vivo*. This could also explain the relative high concentrations of metformin required to achieve a biological response in HNSCC cells *in vitro*, although this can be also explained by the low levels of transporters involved in metformin incorporation into cells *in vitro* (35). The decrease in circulating insulin and IGF-1 appears to be particularly relevant for lung cancer models, in which the high sucrose diet utilized and/or distinct mice strain may sensitize the mice to the IGF-1 and insulin lowering activity of metformin, as recently reported (35). On the other hand, the best-studied direct action of metformin involves the inhibition of mitochondrial complex I and the

consequent activation of AMPK upon increased cellular AMP levels (19). Indeed, we observed that HNSCC cells exposed to metformin display reduced levels of ATP, and increased levels of active AMPK and of the phosphorylated form of its direct downstream target, ACC. However, the activation of AMPK requires its phosphorylation by the upstream tumor suppressor serine/threonine kinase LKB1 (20). Knock down of LKB1 in HNSCC cells and the use of cervical SCCs that do not express LKB1 revealed that this kinase, and hence AMPK activation, may not be strictly required to diminish mTORC1 function in response to metformin. Similar observations were recently reported in prostate cancer cells, in which the authors described a novel mechanism by which metformin blocks mTORC1 by activating the expression of the mTOR inhibitor known as REDD1 (36). However, in this case REDD1 expression involves a p53-dependent pathway, which is triggered by metformin in this tumor type (36). As most HNSCC exhibit p53 mutations or functional inactivation of this tumor suppressor, for example by HPV encoded E6 proteins in HPV-associated HNSCC and cervical SCC (37), this recently described p53-REDD1 axis blocking mTORC1 may not be functional in HNSCC. Alternatively, metformin may stimulate REDD1 expression by a yet to be identified transcriptional program, or inhibit mTORC1 by additional mechanism such as those recently described impinging on Rag GTPases (38). Certainly, the appreciation of the complexity of the molecular mechanisms perturbed by metformin has increased over the past few years, and we can envision that further work may soon help dissect the precise AMPK-dependent and – independent pathways by which metformin regulate mTORC1 function in HNSCC cells and their preneoplastic precursors, and the relative contribution of circulating IGF-1 and insulin in this process.

Similar to the pathogenesis of most solid tumors, squamous cell carcinomas of the head and neck are often associated with a multistage process that requires the progressive acquisition of genetic and epigenetic alterations. In the particular case of HNSCC tumors, which are largely diagnosed in the oral cavity and pharynx, these changes are generally triggered by the chronic exposure to carcinogenic substances associated with chronic tobacco use or betel nut chewing (39, 40). During this multistep carcinogenesis, it is not uncommon that premalignant lesions clinically evident as leukoplakias or erythroplakias reveal dysplastic cellular changes susceptible to malignant transformation (32). Although, it is predicted that the rate of malignant conversion of epithelial dysplasias is relatively low (10-15%), it would be highly desirable to target these lesions to halt tumor progression and ultimately prevent the increased morbidity associated with HNSCC, which greatly impacts patient overall prognosis and survival. Continuing efforts to elucidate key cellular and molecular abnormalities underlying the pathogenesis of HNSCC are now shedding light into the development of novel molecularly-targeted approaches for HNSCC prevention and treatment.

In this regard, the notion of using a FDA-approved drug like metformin as a chemopreventive agent to control oral carcinogenesis is definitely appealing. Although in our studies we used metformin delivered by ip injection to ensure a precise dose, similar results were obtained in preliminary studies when metformin was administered through water consumption, as reported in lung cancer animal models (35). Thus, these studies could be considered as a proof of principle aimed at utilizing orally available drugs, such as metformin, in at risk patients. Indeed, because of its well-accepted safety profile and tolerance relative to its long-term use, metformin may become an attractive chemopreventive agent to hamper the progression of premalignant lesions highly dependent on mTORC1 activity. In addition prolonged metformin administration may also decrease the recurrence rate of previously resected tumors, as it may prevent the malignant conversion of sub-clinical lesions involving epithelial cells harboring genetic alterations caused, for example, by prolonged exposure to tobacco carcinogens in the same field than the primary

HNSCC lesion. Overall, while additional future studies may help define how metformin decreases mTORC1 activity in oral epithelial cells, our present results may provide a strong rationale for the early evaluation of metformin and related agents for oral cancer prevention in its at risk patient population.

Supplementary Material

Refer to Web version on PubMed Central for supplementary material.

Acknowledgments

This article was supported by the Intramural Research Program of the National Institutes of Health, National Institute of Dental and Craniofacial Research, project Z01DE00558, and by the University of Maryland (RHY and AS).

T.M. was supported in part by a JSPS Research Fellowship for Japanese Biomedical and Behavioral Researchers at NIH.

References

1. Siegel R, Ward E, Brawley O, Jemal A. Cancer statistics, 2011: the impact of eliminating socioeconomic and racial disparities on premature cancer deaths. *CA Cancer J Clin.* 2011; 61:212–36. [PubMed: 21685461]
2. Amornphimoltham P, Patel V, Sodhi A, Nikitakis NG, Sauk JJ, Sausville EA, et al. Mammalian target of rapamycin, a molecular target in squamous cell carcinomas of the head and neck. *Cancer Res.* 2005; 65:9953–61. [PubMed: 16267020]
3. Molinolo AA, Hewitt SM, Amornphimoltham P, Keelawat S, Rangdaeng S, Meneses Garcia A, et al. Dissecting the Akt/mammalian target of rapamycin signaling network: emerging results from the head and neck cancer tissue array initiative. *Clin Cancer Res.* 2007; 13:4964–73. [PubMed: 17785546]
4. Nathan CO, Amirghahari N, Rong X, Giordano T, Sibley D, Nordberg M, et al. Mammalian target of rapamycin inhibitors as possible adjuvant therapy for microscopic residual disease in head and neck squamous cell cancer. *Cancer Res.* 2007; 67:2160–8. [PubMed: 17332346]
5. Patel V, Marsh CA, Dorsam RT, Mikelis CM, Masedunskas A, Amornphimoltham P, et al. Decreased Lymphangiogenesis and Lymph Node Metastasis by mTOR Inhibition in Head and Neck Cancer. *Cancer Res.* 2011
6. Agrawal N, Frederick MJ, Pickering CR, Bettegowda C, Chang K, Li RJ, et al. Exome sequencing of head and neck squamous cell carcinoma reveals inactivating mutations in NOTCH1. *Science.* 2011; 333:1154–7. [PubMed: 21798897]
7. Stransky N, Egloff AM, Tward AD, Kostic AD, Cibulskis K, Sivachenko A, et al. The mutational landscape of head and neck squamous cell carcinoma. *Science.* 2011; 333:1157–60. [PubMed: 21798893]
8. Massarelli E, Liu DD, Lee JJ, El-Naggar AK, Lo Muzio L, Staibano S, et al. Akt activation correlates with adverse outcome in tongue cancer. *Cancer.* 2005; 104:2430–6. [PubMed: 16245318]
9. Molinolo AA, Amornphimoltham P, Squarize CH, Castilho RM, Patel V, Gutkind JS. Dysregulated molecular networks in head and neck carcinogenesis. *Oral Oncol.* 2009; 45:324–34. [PubMed: 18805044]
10. Sengupta S, Peterson TR, Laplante M, Oh S, Sabatini DM. mTORC1 controls fasting-induced ketogenesis and its modulation by ageing. *Nature.* 2010; 468:1100–4. [PubMed: 21179166]
11. Zoncu R, Efeyan A, Sabatini DM. mTOR: from growth signal integration to cancer, diabetes and ageing. *Nat Rev Mol Cell Biol.* 2011; 12:21–35. [PubMed: 21157483]
12. Bodmer M, Meier C, Krahenbuhl S, Jick SS, Meier CR. Long-term metformin use is associated with decreased risk of breast cancer. *Diabetes Care.* 2010; 33:1304–8. [PubMed: 20299480]

13. Bowker SL, Majumdar SR, Veugelers P, Johnson JA. Increased cancer-related mortality for patients with type 2 diabetes who use sulfonylureas or insulin. *Diabetes Care*. 2006; 29:254–8. [PubMed: 16443869]
14. Evans JM, Donnelly LA, Emslie-Smith AM, Alessi DR, Morris AD. Metformin and reduced risk of cancer in diabetic patients. *Bmj*. 2005; 330:1304–5. [PubMed: 15849206]
15. Ben Sahra I, Le Marchand-Brustel Y, Tanti JF, Bost F. Metformin in cancer therapy: a new perspective for an old antidiabetic drug? *Mol Cancer Ther*. 2010; 9:1092–9. [PubMed: 20442309]
16. Pollak M. Metformin and other biguanides in oncology: advancing the research agenda. *Cancer Prev Res (Phila)*. 2010; 3:1060–5. [PubMed: 20810670]
17. Dowling RJ, Zakikhani M, Fantus IG, Pollak M, Sonenberg N. Metformin inhibits mammalian target of rapamycin-dependent translation initiation in breast cancer cells. *Cancer Res*. 2007; 67:10804–12. [PubMed: 18006825]
18. Zakikhani M, Dowling R, Fantus IG, Sonenberg N, Pollak M. Metformin is an AMP kinase-dependent growth inhibitor for breast cancer cells. *Cancer Res*. 2006; 66:10269–73. [PubMed: 17062558]
19. El-Mir MY, Nogueira V, Fontaine E, Averet N, Rigoulet M, Leverve X. Dimethylbiguanide inhibits cell respiration via an indirect effect targeted on the respiratory chain complex I. *J Biol Chem*. 2000; 275:223–8. [PubMed: 10617608]
20. Shaw RJ, Lamia KA, Vasquez D, Koo SH, Bardeesy N, Depinho RA, et al. The kinase LKB1 mediates glucose homeostasis in liver and therapeutic effects of metformin. *Science*. 2005; 310:1642–6. [PubMed: 16308421]
21. Inoki K, Li Y, Xu T, Guan KL. Rheb GTPase is a direct target of TSC2 GAP activity and regulates mTOR signaling. *Genes Dev*. 2003; 17:1829–34. [PubMed: 12869586]
22. Czerninski R, Amornphimoltham P, Patel V, Molinolo AA, Gutkind JS. Targeting mammalian target of rapamycin by rapamycin prevents tumor progression in an oral-specific chemical carcinogenesis model. *Cancer Prev Res (Phila)*. 2009; 2:27–36. [PubMed: 19139015]
23. Castilho RM, Squarize CH, Leelahavanichkul K, Zheng Y, Bugge T, Gutkind JS. Rac1 is required for epithelial stem cell function during dermal and oral mucosal wound healing but not for tissue homeostasis in mice. *PLoS One*. 2010; 5:e10503. [PubMed: 20463891]
24. Wang FQ, Ariztia EV, Boyd LR, Horton FR, Smicun Y, Hetherington JA, et al. Lysophosphatidic acid (LPA) effects on endometrial carcinoma in vitro proliferation, invasion, and matrix metalloproteinase activity. *Gynecol Oncol*. 2010; 117:88–95. [PubMed: 20056268]
25. Schneider A, Younis RH, Gutkind JS. Hypoxia-induced energy stress inhibits the mTOR pathway by activating an AMPK/REDD1 signaling axis in head and neck squamous cell carcinoma. *Neoplasia*. 2008; 10:1295–302. [PubMed: 18953439]
26. Maruyama T, Kono K, Mizukami Y, Kawaguchi Y, Mimura K, Watanabe M, et al. Distribution of Th17 cells and FoxP3(+) regulatory T cells in tumor-infiltrating lymphocytes, tumor-draining lymph nodes and peripheral blood lymphocytes in patients with gastric cancer. *Cancer Sci*. 2010; 101:1947–54. [PubMed: 20550524]
27. Ben Sahra I, Laurent K, Loubat A, Giorgetti-Peraldi S, Colosetti P, Auberger P, et al. The antidiabetic drug metformin exerts an antitumoral effect in vitro and in vivo through a decrease of cyclin D1 level. *Oncogene*. 2008; 27:3576–86. [PubMed: 18212742]
28. Cantrell LA, Zhou C, Mendivil A, Malloy KM, Gehrig PA, Bae-Jump VL. Metformin is a potent inhibitor of endometrial cancer cell proliferation—implications for a novel treatment strategy. *Gynecol Oncol*. 2010; 116:92–8. [PubMed: 19822355]
29. Zhou G, Myers R, Li Y, Chen Y, Shen X, Fenyk-Melody J, et al. Role of AMP-activated protein kinase in mechanism of metformin action. *J Clin Invest*. 2001; 108:1167–74. [PubMed: 11602624]
30. Tiainen M, Ylikorkala A, Makela TP. Growth suppression by Lkb1 is mediated by a G(1) cell cycle arrest. *Proc Natl Acad Sci U S A*. 1999; 96:9248–51. [PubMed: 10430928]
31. Vitale-Cross L, Czerninski R, Amornphimoltham P, Patel V, Molinolo AA, Gutkind JS. Chemical carcinogenesis models for evaluating molecular-targeted prevention and treatment of oral cancer. *Cancer Prev Res (Phila)*. 2009; 2:419–22. [PubMed: 19401522]

32. Warnakulasuriya S, Reibel J, Bouquot J, Dabelsteen E. Oral epithelial dysplasia classification systems: predictive value, utility, weaknesses and scope for improvement. *J Oral Pathol Med*. 2008; 37:127–33. [PubMed: 18251935]
33. Argiris A, Karamouzis MV, Raben D, Ferris RL. Head and neck cancer. *Lancet*. 2008; 371:1695–709. [PubMed: 18486742]
34. Klass CM, Shin DM. Current status and future perspectives of chemoprevention in head and neck cancer. *Curr Cancer Drug Targets*. 2007; 7:623–32. [PubMed: 18045067]
35. Goodwin PJ, Ligibel JA, Stambolic V. Metformin in breast cancer: time for action. *J Clin Oncol*. 2009; 27:3271–3. [PubMed: 19487373]
36. Ben Sahra I, Regazzetti C, Robert G, Laurent K, Le Marchand-Brustel Y, Auberger P, et al. Metformin, independent of AMPK, induces mTOR inhibition and cell-cycle arrest through REDD1. *Cancer Res*. 2011; 71:4366–72. [PubMed: 21540236]
37. Scheffner M, Werness BA, Huibregtse JM, Levine AJ, Howley PM. The E6 oncoprotein encoded by human papillomavirus types 16 and 18 promotes the degradation of p53. *Cell*. 1990; 63:1129–36. [PubMed: 2175676]
38. Kalender A, Selvaraj A, Kim SY, Gulati P, Brule S, Viollet B, et al. Metformin, independent of AMPK, inhibits mTORC1 in a rag GTPase-dependent manner. *Cell Metab*. 2010; 11:390–401. [PubMed: 20444419]
39. Forastiere A, Koch W, Trotti A, Sidransky D. Head and neck cancer. *N Engl J Med*. 2001; 345:1890–900. [PubMed: 11756581]
40. Mao L, Hong WK, Papadimitrakopoulou VA. Focus on head and neck cancer. *Cancer Cell*. 2004; 5:311–6. [PubMed: 15093538]

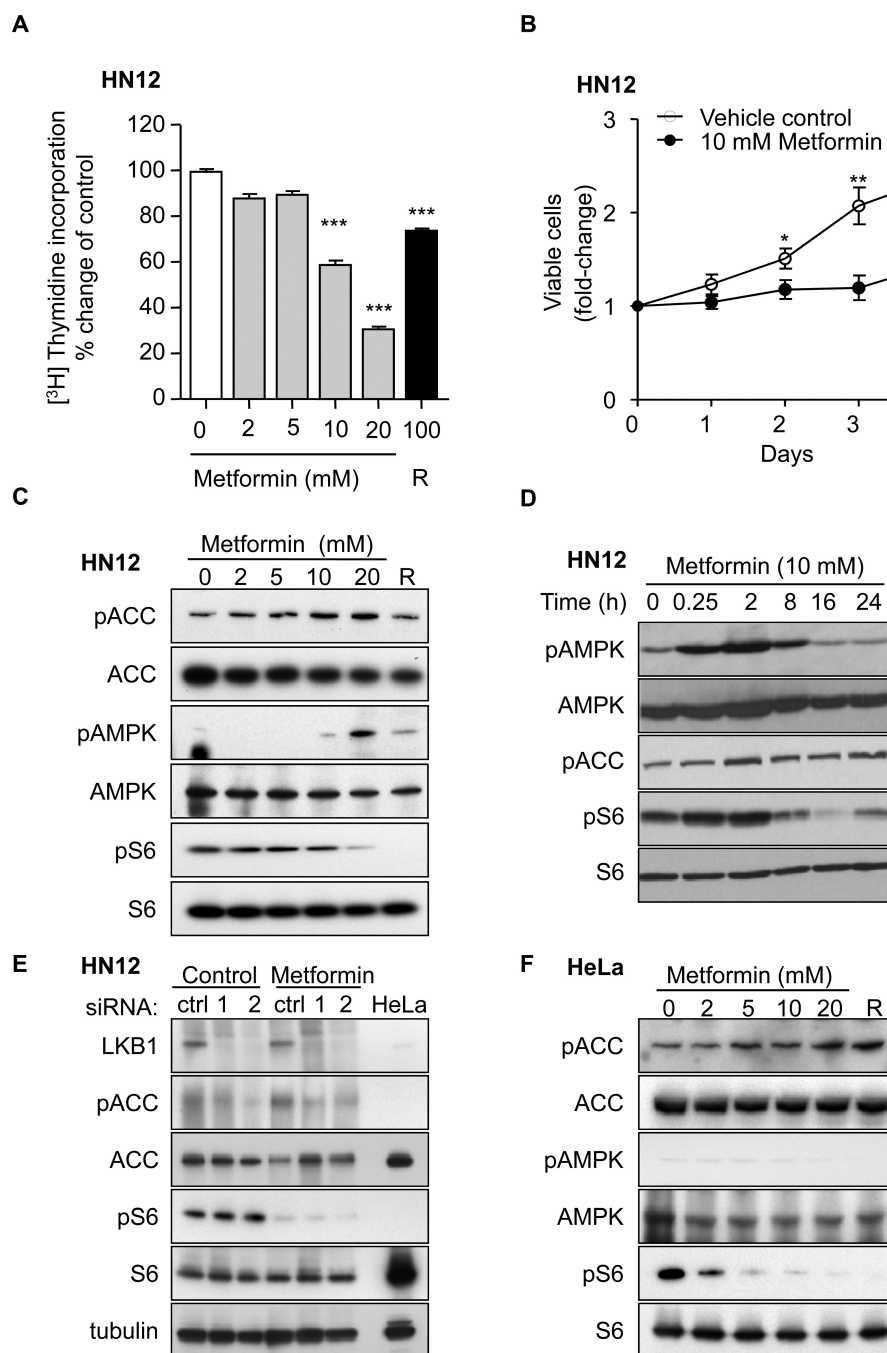


Figure 1. Metformin induces HNSCC cell growth inhibition and reduces mTORC1 activity in an AMPK-independent manner

(A) Cell proliferation was assessed in HN12 cells treated with increasing doses of metformin or 100 nM rapamycin (R) by [³H]-thymidine incorporation as described in *Material and Methods*. *** $p < 0.01$, vehicle- versus metformin-treated cells or rapamycin-treated cells. (B) HN12 cell viability was assessed by the MTS colorimetric assay daily for 4 days. * $p < 0.05$, ** $p < 0.01$ vehicle- versus metformin-treated cells. (C, D) Western blot analysis to evaluate the dose- (C) and time- (D) dependent effects of metformin on the AMPK and mTORC1 pathways in HN12 cells, respectively. R: 100 nM rapamycin as positive control for mTORC1 pathway inhibition. (E) Western blotting to demonstrate the effects of the LKB1/

AMPK signaling pathway on the response to metformin. Following transfections with a control siRNA (ctl) or LKB1 siRNAs (1 and 2), 10 mM metformin was added to HN12 cells for 24 hours. LKB1 RNA interference was performed as described in *Materials and Methods*. HeLa cells were used as positive controls to show lack of endogenous LKB1 activity. (F) Western blotting to assess the LKB1-independent effect of the indicated doses of metformin on the AMPK and mTORC1 pathways in HeLa cells.

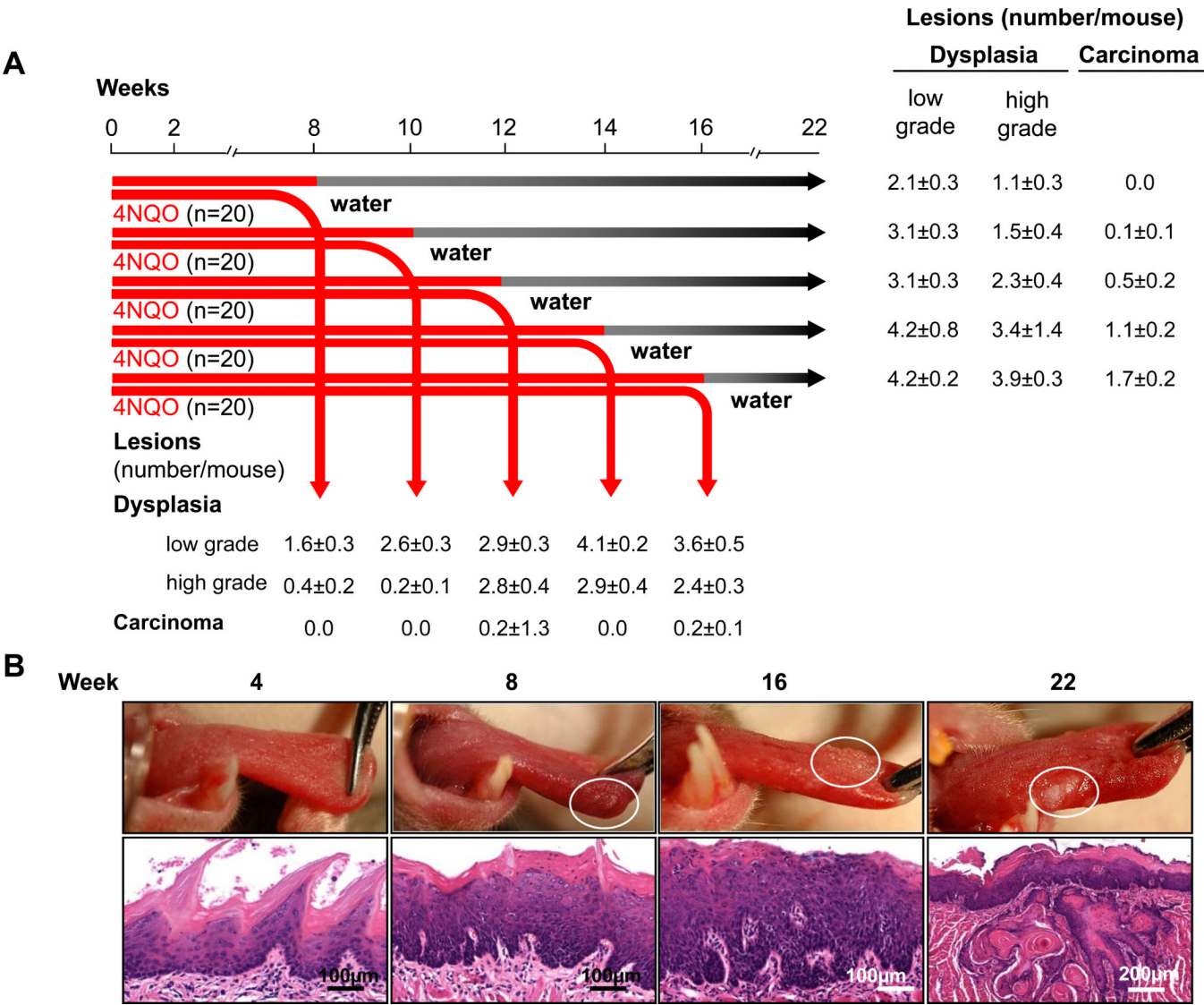


Figure 2. Optimization scheme of the 4NQO oral-specific chemical carcinogenesis model demonstrates time-dependent malignant progression of oral epithelial dysplastic lesions

A. The indicated groups of mice (n=20) were randomly divided and administered with 4NQO in the drinking water (50 µg/ml) for the indicated time (8, 10, 12, 14, and 16 weeks). Mice were then sacrificed or switched to regular water, and sacrificed at week 22 from the initiation of the 4NQO administration. The tongue of each mouse was processed for detailed histological examination as described in Materials and Methods. The average of the number of lesions per mouse, classified as low grade dysplasia, high grade dysplasia, or carcinoma based on histopathological examination was recorded at the end of the 4NQO administration as well as on week 22 from the initiation of carcinogen exposure. B, representative pictures of lesions observed in mice at the indicated time since the initiation of carcinogen exposure in mice treated with 4NQO for 14 weeks. No evident gross alteration were observed at week 4; small elevated white lesions and discoloration are seen at week 8; the lesions grow to small berry-like elevations at week 16 and to ill-defined indurated white or congestive areas, often ulcerated, at week 22. Microscopically, the series of picture depict the sequence of histological changes on the dorsal tongue from a normal epithelium at week 4, through mild to moderate atypia at week 8, several dysplastic cellular alterations at week 16 (note

the increasing thickness of the epithelium), to a fully infiltrating well differentiated squamous cell carcinoma at week 22.

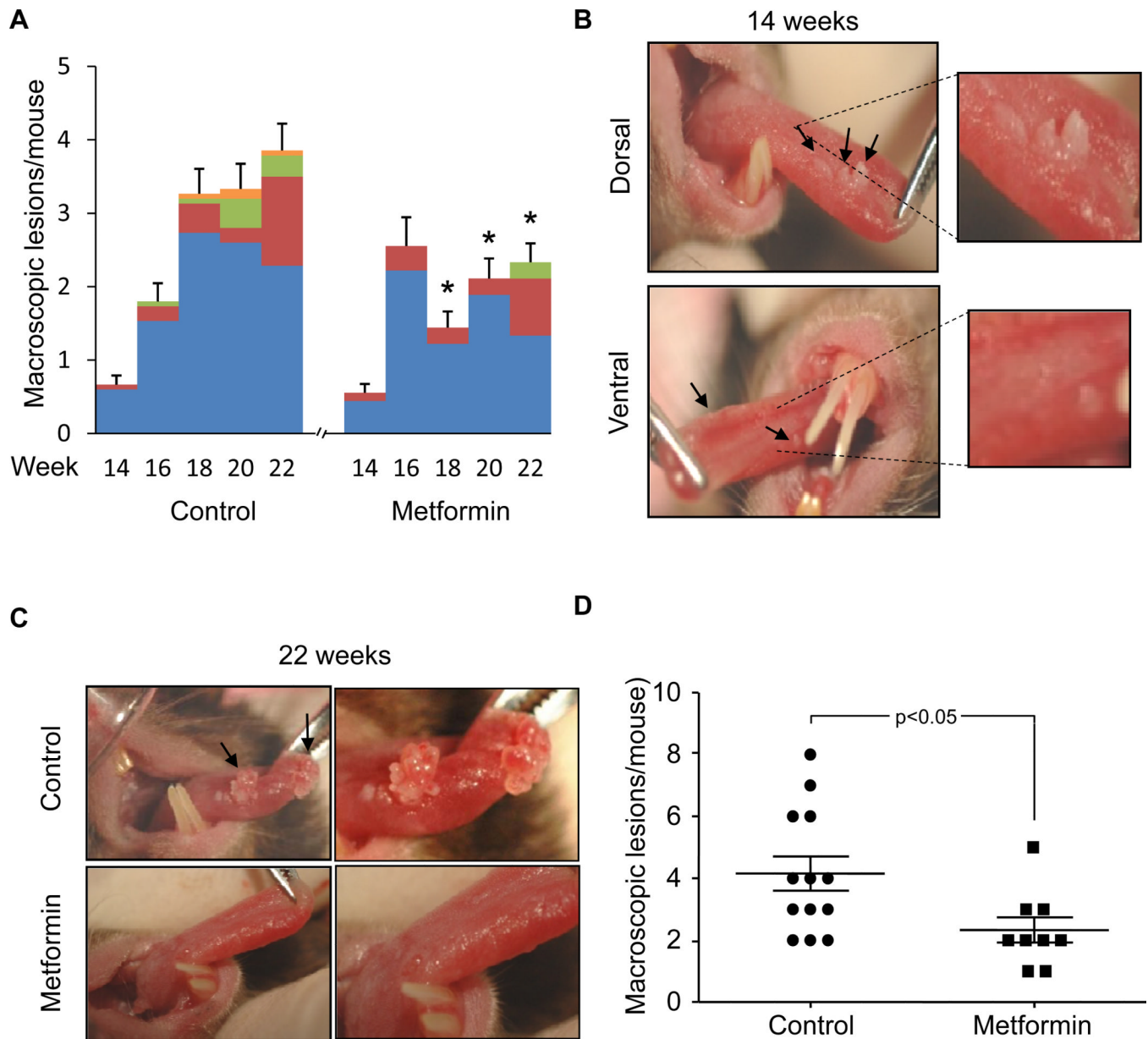


Figure 3. Metformin decreases the number and size of oral tumors induced by orally-administered 4NQO carcinogen

(A) C57Bl/6 mice were administered 4NQO diluted in the drinking water for 14 weeks, as described in Materials and Methods, and remained on regular water until week 22. At week 14, the mice were divided into 2 groups and given either daily i.p. injections of metformin at a dose of 50 mg/kg/day or an equal volume of sterile saline for a period of 8 weeks. Grossly evident lesions started to appear by week 16, and by week 18 the difference between metformin-treated and untreated groups was significant. In panel A, the cumulative incidence of the number of macroscopic lesions per animal is shown; the different colors indicate their respective size: 2-4mm (blue), 4-6mm (orange), 6-8mm (green), 8-10mm (red). (B) Gross morphology of the lesions developed in the animals treated with 4NQO in the metformin-treated and control untreated groups. At week 14, when 4NQO treatment was stopped, the alterations are more evident in the dorsal tongue. A rather extensive white and elevated tumor composed of three different outgrowths is evident in this control animal

(arrow, left uppermost picture). Smaller lesions are seen in the ventral aspect of the tongue (arrow, lower rightmost picture). (C) At week 22, an untreated control animal has developed a significant papillomatous tumor in the middle the tongue as well as another similar lesion in the tip of the organ (arrows). Only small discolorations are observed in an animal treated with metformin. In the ventral tongue the control animal has developed two evident berry-like outgrowths, while only one small white papillomatous lesion is seen in the metformin-treated animal (arrows). (D) At the conclusion of the experimental period (week 22), the difference in the incidence of tumor lesions per animal was evident between metformin- and control-treated mice is significant.

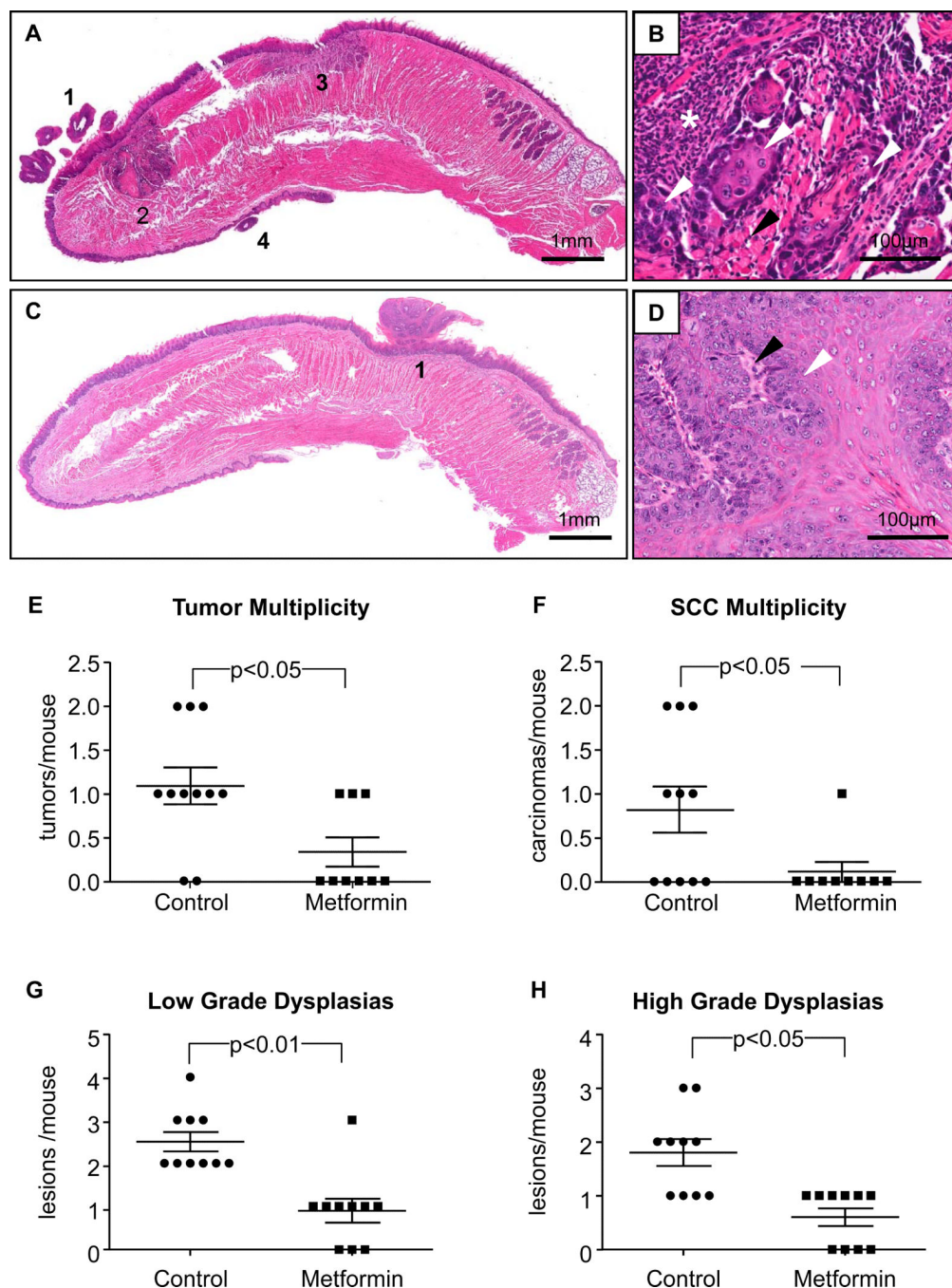


Figure 4. Metformin decreases the number and size of oral tumors, and prevents the malignant conversion of preneoplastic lesions

(A) A sagittal section of a tongue in a control animal at week 22 after the initiation of the exposure to 4NQO in the drinking water for 14 weeks, where a total of 3 tumors are observed. The lesion closest to the tip of the tongue has a papillary (1) as well as a clearly infiltrative aspect (2); closer to the middle of the dorsal tongue another infiltrative squamous cell carcinoma is evident (3). The third tumor, a papilloma, is observed in the ventral tongue (4). (B) A higher magnification of lesion 2; atypical epithelial cells showing squamous differentiation (white arrow head) infiltrate the skeletal muscle of the tongue (black arrow head). They are surrounded by a dense inflammatory infiltrate (white star). (C) In this

metformin-treated animal a single large benign papillomatous lesion is seen in the posterior dorsal tongue (1) (D) At a higher magnification, the squamous epithelium (white arrow head) lines thin projections of the stroma (black arrow head), it is evidently hyperplastic, although the cells display no evident atypia; mitotic figures are not evident in this picture. E and F. Tumor multiplicity, including benign and malignant tumors (E) as well as SCC multiplicity (F) are significantly different between metformin-treated and untreated control groups. G and F. The number of preneoplastic lesions per tongue, both low and high grade dysplasias was also significantly reduced in the metformin treated animals.

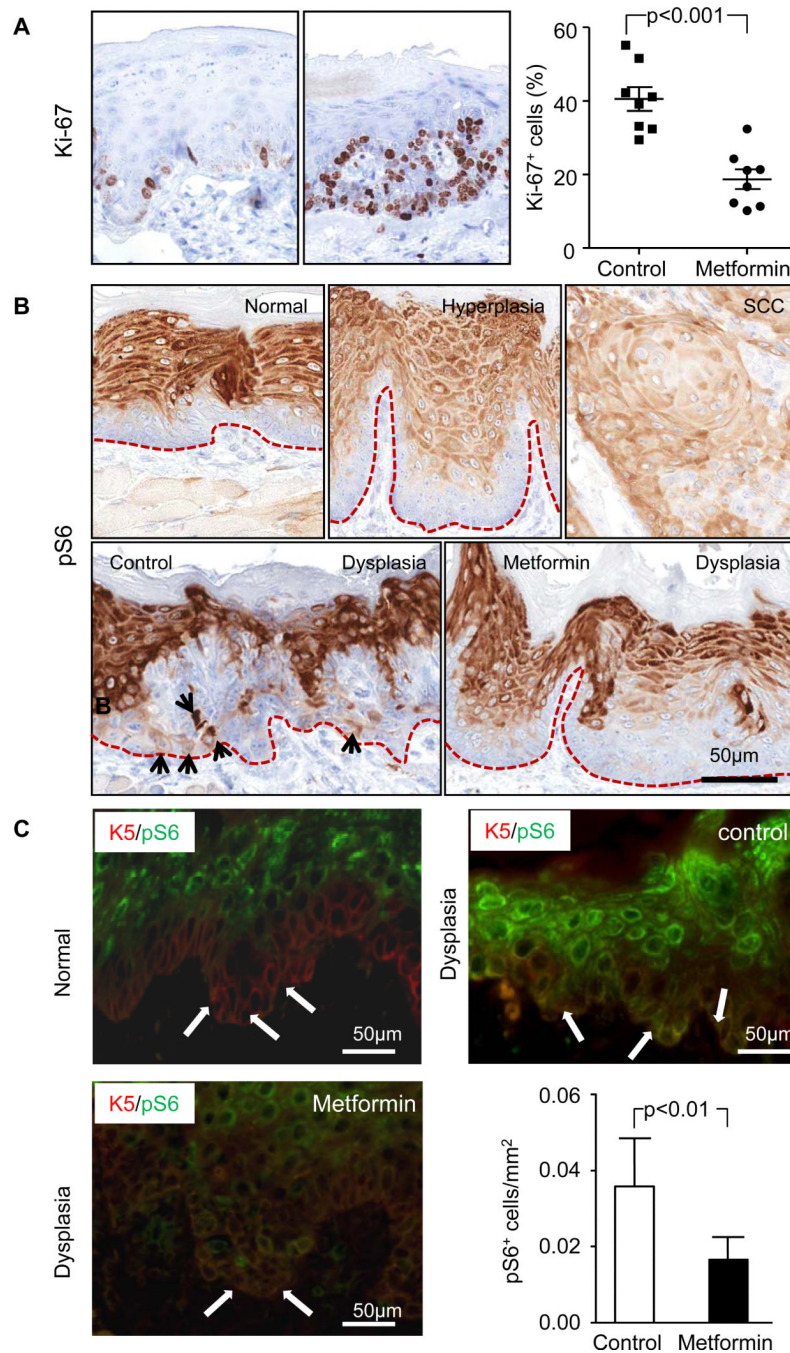


Figure 5. Metformin decreases mTORC1 activity in the basal layer of oral epithelial dysplasias, and mitotic activity in the hyperplastic epithelium

(A) The percentage of proliferating cells was evaluated in hyperplastic tongue epithelium using a Ki-67 rat monoclonal antibody. The animals treated with metformin show a significantly lower level of proliferating cells as compared with the control. Representative images showing nuclear immunoreactivity for Ki-67 in metformin (left) and metformin-treated animals (right) as well as the quantification are shown in the figure. (B) Positive immunoreactivity to the mTORC1 downstream target pS6 in normal (normal) and hyperplastic (hyperplasia) tissues is limited to the upper layers of the squamous epithelium of the dorsal tongue (upper panels). The rightmost picture shows dysregulated expression in

a squamous cell carcinoma (SCC). Most of the cells express pS6, regardless of their degree of differentiation. Conversely, increased pS6 expression is clearly evident in premalignant dysplastic lesions developed in control animals treated for 14 weeks with 4NQO (dysplasia), where pS6 immunoreactivity appears on the basal and suprabasal epithelium (arrowheads), underscoring a decompartmentalization of mTORC1 activity within the proliferating epithelial layers (lower left panel). One of the most interesting effects induced by metformin treatment is that it restores pS6 expression to the upper compartment of the squamous epithelium, far from the actively proliferating compartment (dysplasia, lower right panel). Indeed, the arrows depict a marked increase in the number of pS6-positive cells in the lower epithelial compartment of dysplastic lesions in control animals in comparison to animals treated with metformin. (C) These differences are more evident following an immunofluorescence double staining, in which pS6 expression (green fluorescence) is limited to the upper differentiated layers of the normal oral epithelium; in fact, no pS6 expression is seen in the basal and parabasal layers where K5 is highly expressed (red fluorescence) (upper left panel) in normal mice. In 4NQO treated animals, the basal layers show a co-expression of both K5 and pS6 within the proliferating compartment as depicted by arrows pointing to yellow immunofluorescent cells (dysplasia, upper right panel). Metformin significantly inhibits the expression of pS6 within the basal layers of mice exposed to 4NQO (dysplasia, lower left panel). Moreover, there is a highly significant difference in the number of pS6-positive cells in the basal layer of the dysplastic lingual epithelium between metformin-treated and control animals exposed to 4NQO as shown in the bar graph (lower right panel).

Table 1
Effect of metformin administration on serum components and immune cell profiles

Mice were administered 4NQO diluted in the drinking water for 14 weeks, divided into 2 groups, and given either daily i.p. injections of metformin at a dose of 50 mg/kg/day or an equal volume of sterile saline for a period of 8 weeks, as described in Figure 3. Mice were euthanized on week 22 from the initiation of 4NQO exposure, and serum and spleen T cells isolated as described in Materials and Methods. Serum components, spleen T cell proliferation, and spleen T cell subtypes were analyzed as described in Materials and Methods. Metformin exerted a very limited impact on serum components and metabolic markers, and did not reduce the T cell proliferative response. Metformin significantly enhanced Th17 cells without changing Th1 and Foxp3+ Tregs, an effect that is under current investigation.

Blood (serum)	Control	Metformin
	n=6	n=6
Glucose (mg/dL)	103.8 ± 14.3	107.3 ± 10.0
Cholesterol (mg/dL)	99.8 ± 9.4	82.2 ± 9.0
Triglycerides (mg/dL)	74.0 ± 9.2	80.3 ± 9.8
Sodium (mmol/L)	153.3 ± 1.0	152.5 ± 1.1
Potassium (mmol/L)	6.9 ± 0.2	7.6 ± 0.5
Chloride (mmol/L)	113.0 ± 2.1	115.2 ± 0.6
Creatinine (mg/dL)	0.1 ± 0.0	0.1 ± 0.0
BUN (mg/dL)	24.2 ± 2.5	21.3 ± 0.9
Calcium (mmol/L)	2.3 ± 0.0	2.3 ± 0.0
Magnesium (mmol/L)	1.3 ± 0.0	1.2 ± 0.0
Phosphorous (mg/dL)	7.9 ± 0.1	8.3 ± 0.3
Alkaline Phosphatase (U/L)	82.5 ± 6.2	88.2 ± 10.5
ALT/GPT (U/L)	125.0 ± 29.7	198.8 ± 56.7
AST/GOT (U/L)	232.0 ± 20.1	248.3 ± 14.3
Amylase (U/L)	±650.0 ± 0.0	±650 ± 0.0
CK, Total (U/L)	±800.0 ± 0.0	±800 ± 0.0
Lact Dehydrogenase (U/L)	±600.0 ± 0.0	±600 ± 0.0
Protein, total (g/dL)	5.3 ± 0.0	5.2 ± 0.2
Uric acid (mg/dL)	3.5 ± 0.0	3.0 ± 0.1

Spleen T cell proliferation	Control	Metformin
	n=8	n=8
media (10 ⁻³ cpm)	3.9 ± 0.5	5.5 ± 1.5
CD3 (10 ⁻³ cpm)	16.5 ± 1.6	27.8 ± 2.9 **

Spleen T cells	Control	Metformin
	n=8	n=8
% total cells labeled		
CD4+	22.9 ± 1.2	16.8 ± 1.5 *
CD8+	29.8 ± 1.5	10.5 ± 1.9 ***
Th1	12.6 ± 1.3	13.4 ± 1.1

Spleen T cells	Control	Metformin
% total cells labeled	n=8	n=8
Th17	1.4 ± 0.1	3.4 ± 0.5 ^{**}
Tregs	26.9 ± 1.1	27.2 ± 1.1

*
p<0.05

**
p<0.01

p<0.001.